

# Input Impedance, VSWR and Return Loss of a Conformal Microstrip Printed Antenna for $TM_{01}$ Mode Using Two Different Substrates

Ali Elrashidi\*, Khaled Elleithy, Hassan Bajwa

Department of Computer and Electrical Engineering, University of Bridgeport, Bridgeport, CT 06604, USA

**Abstract** Curvature has a great effect on fringing field of a microstrip antenna and consequently fringing field affects effective dielectric constant and then all antenna parameters. A new mathematical model for input impedance, return loss and voltage standing wave ratio is introduced in this paper. These parameters are given for  $TM_{01}$  mode and using two different substrate materials K-6098 Teflon/Glass and Epsilam-10 Ceramic-Filled Teflon materials.

**Keywords** Fringing Field, Curvature, Effective Dielectric Constant and Return Loss (S11), Voltage Standing Wave Ratio (VSWR), Transverse Magnetic  $TM_{01}$  Mode

## 1. Introduction

Due to the unprinted growth in wireless applications and increasing demand of low cost solutions for **RF** and microwave **communication** systems, the microstrip flat antenna, has **undergone** tremendous growth recently. Though the models used in analyzing microstrip structures have been widely accepted, the effect of curvature on dielectric constant and antenna performance has not been studied in detail. Low profile, low weight, low cost and its ability of conforming to curve surfaces[1], conformal microstrip structures have also witnessed enormous growth in the last few years. Applications of microstrip structures include Unmanned Aerial Vehicle (UAV), planes, rocket, radars and communication industry[2]. Some advantages of conformal antennas over the planer microstrip structure include, easy installation (random not needed), capability of embedded structure within composite aerodynamic surfaces, better angular coverage and controlled gain, depending upon shape[3,4]. While Conformal Antenna provide potential solution for many applications, it has some drawbacks due to bedding[5]. Such drawbacks include phase, impedance, and resonance frequency errors due to the stretching and compression of the dielectric material along the inner and outer surfaces of conformal surface. Changes in the dielectric constant and material thickness also affect the performance of the antenna. Analysis tools for conformal arrays are not mature and fully developed[6].

Dielectric materials suffer from cracking due to bending and that will affect the performance of the conformal microstrip antenna.

## 2. Background

Conventional microstrip antenna has a metallic patch printed on a thin, grounded dielectric substrate. Although the patch can be of any shape, rectangular patches, as shown in Figure 1 [7], are preferred due to easy calculation and modeling.

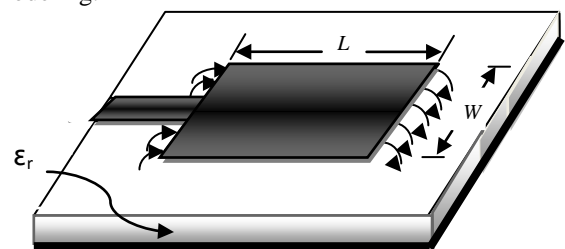


Figure 1. Rectangular microstrip antenna.

Fringing fields have a great effect on the performance of a microstrip antenna. In microstrip antennas the electric field in the center of the patch is zero. The radiation is due to the fringing field between the periphery of the patch and the ground plane. For the rectangular patch shown in the Figure 2, there is no field variation along the width and thickness. The amount of the fringing field is a function of the dimensions of the patch and the height of the substrate. Higher the substrate, the greater is the fringing field.

Due to the effect of fringing, a microstrip patch antenna would look electrically wider compared to its physical dimensions. As shown in Figure 2, waves travel both in sub-

\* Corresponding author:

aelrashidi@bridgeport.edu (Ali Elrashidi)

Published online at <http://journal.sapub.org/ijnc>

Copyright © 2012 Scientific & Academic Publishing. All Rights Reserved

strate and in the air. Thus an effective dielectric constant  $\epsilon_{\text{reff}}$  is to be introduced. The effective dielectric constant  $\epsilon_{\text{reff}}$  takes in account both the fringing and the wave propagation in the line.

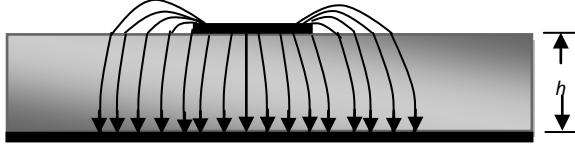


Figure 2. Electric field lines (Side View).

The expression for the effective dielectric constant is introduced by A. Balanis[7], as shown in Equation 1.

$$\epsilon_{\text{reff}} = \frac{\epsilon_r + 1}{2} + \frac{\epsilon_r - 1}{2} \left[ 1 + 12 \frac{h}{w} \right]^{-\frac{1}{2}} \quad (1)$$

The length of the patch is extended on each end by  $\Delta L$  is a function of effective dielectric constant  $\epsilon_{\text{reff}}$  and the width to height ratio ( $W/h$ ).  $\Delta L$  can be calculated according to a practical approximate relation for the normalized extension of the length [8], as in Equation 2.

$$\frac{\Delta L}{h} = 0.412 \frac{(\epsilon_{\text{reff}} + 0.3) \left( \frac{w}{h} + 0.264 \right)}{(\epsilon_{\text{reff}} - 0.258) \left( \frac{w}{h} + 0.8 \right)} \quad (2)$$

The effective length of the patch is  $L_{\text{eff}}$  and can be calculated as in Equation 3.

$$L_{\text{eff}} = L + 2\Delta L \quad (3)$$

By using the effective dielectric constant (Equation 1) and effective length (Equation 3), we can calculate the resonance frequency of the antenna  $f$  and all the microstrip antenna parameters.

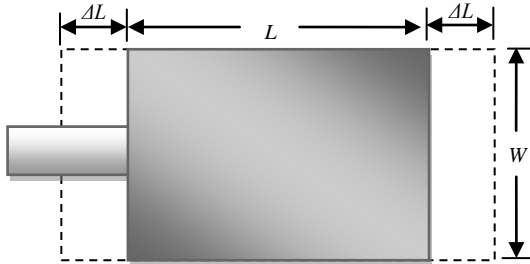


Figure 3. Physical and effective lengths of rectangular microstrip patch.

### Cylindrical-Rectangular Patch Antenna

All the previous work for a conformal rectangular microstrip antenna assumed that the curvature does not affect the effective dielectric constant and the extension on the length. The effect of curvature on the resonant frequency has been presented previously[9]. In this paper we present the effect of fringing field on the performance of a conformal patch antenna. A mathematical model that includes the effect of curvature on fringing field and on antenna performance is presented. The cylindrical rectangular patch is the most famous and popular conformal antenna. The manufacturing of this antenna is easy with respect to spherical and conical

antennas.

Effect of curvature of conformal antenna on resonant frequency been presented by Clifford M. Krowne[9,10] as:

$$[(f)_r]_{mn} = \frac{1}{2\sqrt{\mu\epsilon}} \sqrt{\left(\frac{m}{20a}\right)^2 + \left(\frac{n}{2b}\right)^2} \quad (4)$$

Where  $2b$  is a length of the patch antenna,  $a$  is a radius of the cylinder,  $2\theta$  is the angle bounded the width of the patch,  $\epsilon$  represents electric permittivity and  $\mu$  is the magnetic permeability as shown in Figure 4.

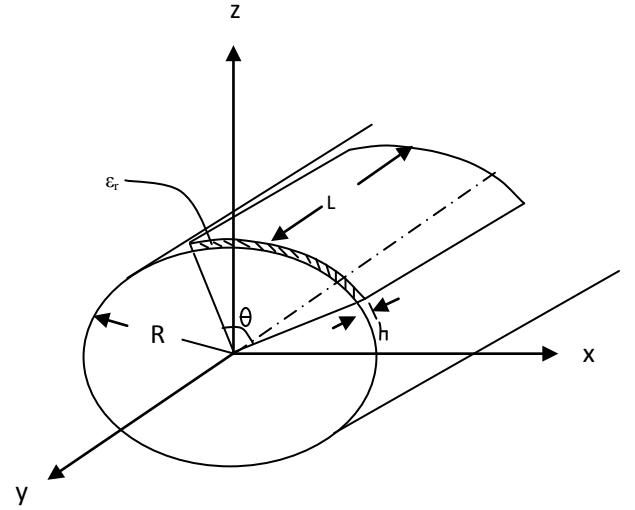


Figure 4. Geometry of cylindrical-rectangular patch antenna[9].

Joseph A. *et al.*, presented an approach to the analysis of microstrip antennas on cylindrical surface. In this approach, the field in terms of surface current is calculated, while considering dielectric layer around the cylindrical body. The assumption is only valid if radiation is smaller than stored energy[11]. Kwai *et al.* [12] gave a brief analysis of a thin cylindrical-rectangular microstrip patch antenna which includes resonant frequencies, radiation patterns, input impedances and  $Q$  factors. The effect of curvature on the characteristics of  $TM_{10}$  and  $TM_{01}$  modes is also presented in Kwai *et al.* paper. The authors first obtained the electric field under the curved patch using the cavity model and then calculated the far field by considering the equivalent magnetic current radiating in the presence of cylindrical surface. The cavity model, used for the analysis is only valid for a very thin dielectric. Also, for much small thickness than a wavelength and the radius of curvature, only  $TM$  modes are assumed to exist. In order to calculate the radiation patterns of cylindrical-rectangular patch antenna. The authors introduced the exact Green's function approach. Using Equation (4), they obtained expressions for the far zone electric field components  $E_\theta$  and  $E_\phi$  as a functions of Hankel function of the second kind  $H_p^{(2)}$ . The input impedance and  $Q$  factors are also calculated under the same conditions.

Based on cavity model, microstrip conformal antenna on a projectile for GPS (Global Positioning System) device is designed and implemented by using perturbation theory is introduced by Sun L., Zhu J., Zhang H. and Peng X[13]. The designed antenna is emulated and analyzed by IE3D software. The emulated results showed that the antenna could provide excellent circular hemisphere beam, better wide-angle circular polarization and better impedance match peculiarity.

Nickolai Zhelev introduced a design of a small conformal microstrip GPS patch antenna[14]. A cavity model and transmission line model are used to find the initial dimensions of the antenna and then electromagnetic simulation of the antenna model using software called FEKO is applied. The antenna is experimentally tested and the author compared the result with the software results. It was founded that the resonance frequency of the conformal antenna is shifted toward higher frequencies compared to the flat one.

The effect of curvature on a fringing field and on the resonance frequency of the microstrip printed antenna is studied in [15]. Also, the effect of curvature on the performance of a microstrip antenna as a function of temperature for  $TM_{01}$  and  $TM_{10}$  is introduced in [16, 17].

### 3. Input Impedance

The input impedance is defined as “the impedance presented by an antenna at its terminals” or “the ratio of the voltage current at a pair of terminals” or “the ratio of the appropriate components of the electric to magnetic fields at a point”. The input impedance is a function of the feeding position as we will see in the next few lines.

To get an expression of input impedance  $Z_{in}$  for the cylindrical microstrip antenna, we need to get the electric field at the surface of the patch. In this case, we can get the wave equation as a function of excitation current density  $J$  as follow:

$$\frac{1}{\rho^2} \frac{\partial^2 E_\rho}{\partial \phi^2} + \frac{\partial^2 E_\rho}{\partial z^2} + k^2 E_\rho = j\omega\mu J \quad (5)$$

By solving this Equation, the electric field at the surface can be expressed in terms of various modes of the cavity as[15]:

$$E_\rho(z, \phi) = \sum_n \sum_m A_{nm} \psi_{nm}(z, \phi) \quad (6)$$

where  $A_{nm}$  is the amplitude coefficients corresponding to the field modes. By applying boundary conditions, homogeneous wave Equation and normalized conditions for  $\psi_{nm}$ , we can get an expression for  $\psi_{nm}$  as shown below:

1.  $\psi_{nm}$  vanishes at the both edges for the length  $L$ :

$$\left. \frac{\partial \psi}{\partial z} \right|_{z=0} = \left. \frac{\partial \psi}{\partial z} \right|_{z=L} = 0 \quad (7)$$

2.  $\psi_{nm}$  vanishes at the both edges for the width  $W$ :

$$\left. \frac{\partial \psi}{\partial \phi} \right|_{\phi=-\theta_1} = \left. \frac{\partial \psi}{\partial \phi} \right|_{\phi=\theta_1} = 0 \quad (8)$$

3.  $\psi_{nm}$  should satisfy the homogeneous wave Equation :

$$\left( \frac{1}{\rho^2} \frac{\partial^2}{\partial \phi^2} + \frac{\partial^2}{\partial z^2} + k^2 \right) \psi_{nm} = 0 \quad (9)$$

4.  $\psi_{nm}$  should satisfy the normalized condition:

$$\int_{z=0}^{z=L} \int_{\phi=-\theta_1}^{\phi=\theta_1} \psi_{nm} \psi_{nm}^* = 1 \quad (10)$$

Hence, the solution of  $\psi_{nm}$  will take the form shown below:

$$\psi_{nm}(z, \phi) = \sqrt{\frac{\epsilon_m \epsilon_n}{2a\theta_1 L}} \cos\left(\frac{m\pi}{2\theta_1}(\phi - \phi_1)\right) \cos\left(\frac{n\pi}{L}z\right) \quad (11)$$

with

$$\epsilon_p = \begin{cases} 1 & \text{for } p = 0 \\ 2 & \text{for } p \neq 0 \end{cases}$$

The coefficient  $A_{nm}$  is determined by the excitation current. For this, substitute Equation (11) into Equation (5) and multiply both sides of (5) by  $\psi_{nm}^*$ , and integrate over area of the patch. Making use of orthonormal properties of  $\psi_{nm}$ , one obtains:

$$A_{nm} = \frac{j\omega\mu}{k^2 - k_{nm}^2} \iint_{dim}^{feed} \psi_{nm}^* J_\rho d\phi dz \quad (12)$$

Now, let the coaxial feed as a rectangular current source with equivalent cross-sectional area  $S_z \times S_\phi$  centered at  $(Z_0, \phi_0)$ , so, the current density will satisfy the Equation below:

$$J_\rho = \begin{cases} \frac{I_0}{S_z S_\phi} & Z_0 - \frac{S_z}{2} \leq x \leq Z_0 + \frac{S_z}{2} \\ & \phi_0 - \frac{S_\phi}{2} \leq x \leq \phi_0 + \frac{S_\phi}{2} \\ 0 & \text{elsewhere} \end{cases} \quad (13)$$

Use of Equation (31) in (30) gives:

$$A_{nm} = \frac{j\omega\mu I}{k^2 - k_{nm}^2} \sqrt{\frac{\epsilon_m \epsilon_n}{2a\theta_1 L}} \cos\left(\frac{m\pi}{2\theta_1}\phi_0\right) \cos\left(\frac{n\pi}{L}Z_0\right) \text{sinc}\left(\frac{n\pi}{2L}Z_0\right) \text{sinc}\left(\frac{m\pi}{2a\theta_1}\phi_0\right) \quad (14)$$

So, to get the input impedance, one can substitute in the following Equation:

$$Z_{in} = \frac{V_{in}}{I_0} \quad (15)$$

where  $V_{in}$  is the *RF* voltage at the feed point and defined as:

$$V_{in} = -E_\rho(z_0, \phi_0) \times h \quad (16)$$

By using Equations (6), (11), (14), (16) and substitute in (15), we can obtain the input impedance for a rectangular microstrip antenna conformal in a cylindrical body as in the following Equation:

$$Z_{in} = \frac{j\omega\mu h \sum_n \sum_m \frac{1}{k^2 - k_{nm}^2} \frac{\epsilon_m \epsilon_n}{2a\theta_1 L} \cos^2\left(\frac{m\pi}{2\theta_1}\phi_0\right) \cos^2\left(\frac{n\pi}{L}Z_0\right)}$$

$$\times \text{sinc}\left(\frac{n\pi}{2L}z_0\right)\text{sinc}\left(\frac{m\pi}{2a\theta_1}\phi_0\right) \quad (17)$$

#### 4. Voltage Standing Wave Ratio and Return Loss

Voltage Standing Wave Ratio  $VSWR$  is defined as the ratio of the maximum to minimum voltage of the antenna. The reflection coefficient  $\rho$  define as a ratio between incident wave amplitude  $V_i$  and reflected voltage wave amplitude  $V_r$ , and by using the definition of a voltage reflection coefficient at the input terminals of the antenna  $\Gamma$ , as shown below:

$$r = \frac{Z_{\text{input}} - Z_0}{Z_{\text{input}} + Z_0} \quad (18)$$

where,  $Z_0$  is the characteristic impedance of the antenna. If the Equation is solved for the reflection coefficient, it is found that, where the reflection coefficient  $\rho$  is the absolute value of the magnitude of  $\Gamma$ ,

$$\rho = |r| = \frac{VSWR - 1}{VSWR + 1} \quad (19)$$

Consequently,

$$VSWR = \frac{|r| + 1}{|r| - 1} \quad (20)$$

The characteristic can be calculated as in [14],

$$Z_0 = \sqrt{\frac{L}{C}} \quad (21)$$

where :  $L$  is the inductance of the antenna, and  $C$  is the capacitance and can be calculated as follow:

$$C = \frac{2\pi\epsilon}{\ln\left(\frac{a+h}{a}\right)} \frac{w}{2\pi\epsilon} \quad (22)$$

$$L = \frac{\mu}{2\pi} \ln\left(\frac{a+h}{a}\right) \frac{w}{2\pi\epsilon} \quad (23)$$

Hence, we can get the characteristic impedance as shown below:

$$Z_0 = \frac{1}{2\pi} \sqrt{\frac{\mu}{\epsilon}} \ln\left(\frac{a+h}{a}\right) \quad (24)$$

The return loss  $S_{11}$  is related through the following Equation:

$$S_{11} = -20\log\left[\frac{V_r}{V_i}\right] = -20\log\left[\frac{VSWR - 1}{VSWR + 1}\right] \quad (25)$$

#### 5. Results

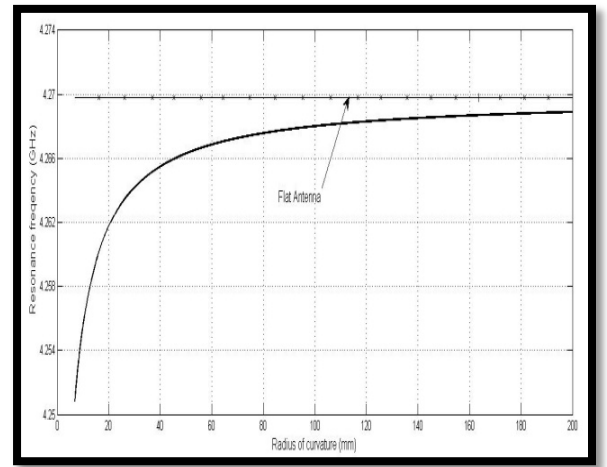
For the range of 2-5 GHz, the dominant modes are  $TM_{01}$  and  $TM_{10}$  for  $h < W$  which is the case. In this paper we concentrate on  $TM_{01}$ . Also, for the antenna operates at the ranges 2.12 and 4.25 GHz for two different substrates we can use the following dimensions; the original length is 20 mm, the width is 23 mm and for different lossy substrate we can get the effect of curvature on the effective dielectric

constant and the resonance frequency.

Two different substrate materials K-6098 Teflon/Glass and Epsilam-10 Ceramic-Filled Teflon are used for verifying the new model. The dielectric constants for the used materials are 2.5 and 10 respectively with a tangent loss 0.002 and 0.004 respectively.

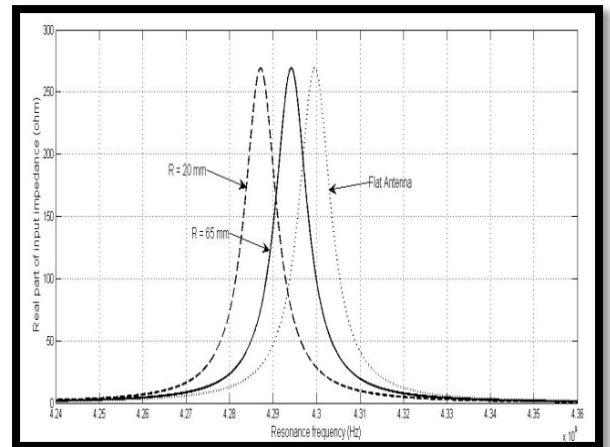
##### 5.1. K-6098 Teflon/Glass Substrate

Figure 5 shows the effect of curvature on resonance frequency for a  $TM_{01}$  mode. The frequency range of resonance frequency due to changing in curvature is from 4.25 to 4.27 GHz for a radius of curvature from 6 mm to flat antenna. So, the frequency is shifted by 20 MHz due to changing in curvature.



**Figure 5.** Resonance frequency as a function of curvature for flat and curved antenna.

The mathematical for input impedance, real and imaginary parts for a different radius of curvatures are shown in Figures 6 and 7. The peak value of the real part of input impedance is almost 270  $\Omega$  at frequency 4.688 GHz which gives a zero value for the imaginary part of input impedance as shown in Figure 7 at 20 mm radius of curvature. The value 4.287 GHz represents a resonance frequency for the antenna at 20 mm radius of curvature.



**Figure 6.** Real part of the input impedance as a function of frequency for different radius of curvatures.

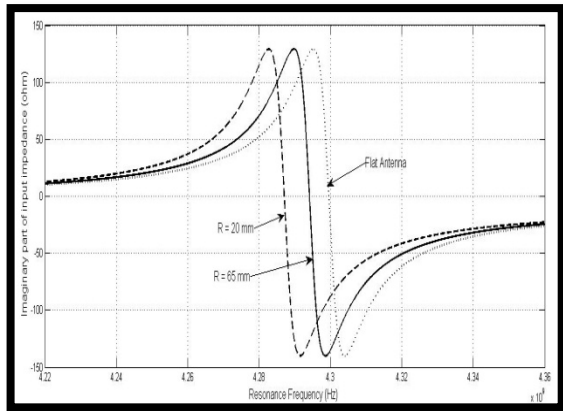


**Figure 7.** Imaginary part of the input impedance as a function of frequency for different radius of curvatures.

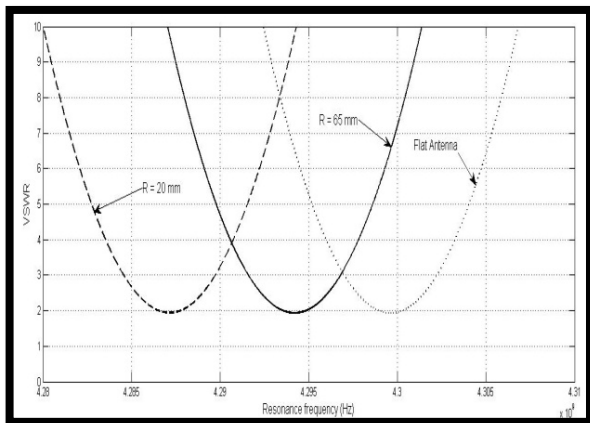


**Figure 8.** VSWR versus frequency for different radius of curvatures.

VSWR is given in Figure 8. It is noted that, the value of VSWR is almost 1.95 at frequency 4.287 GHz which is very efficient in manufacturing process. It should be between 1 and 2 for radius of curvature 20 mm. The minimum VSWR we can get, the better performance we can obtain as shown clearly from the definition of VSWR.

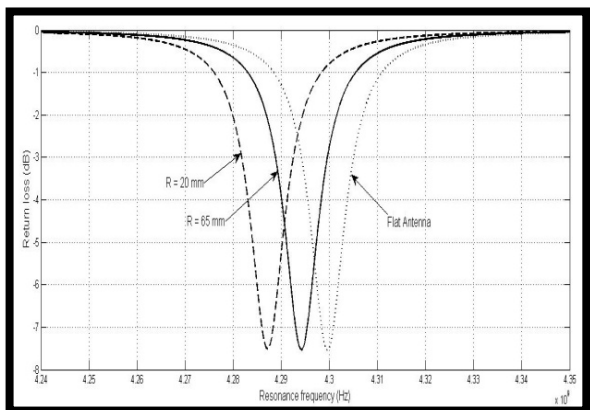
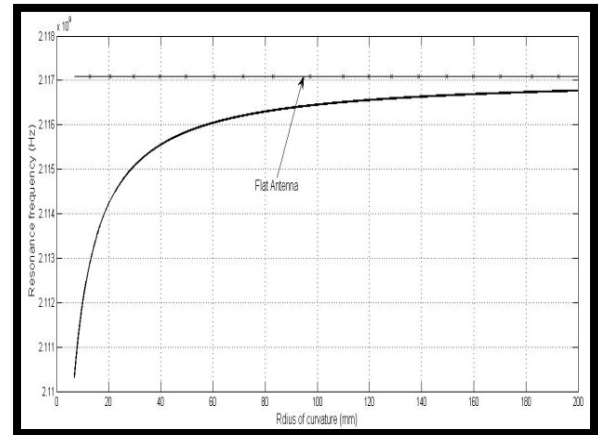


**Figure 9.** Return loss (S11) as a function of frequency for different radius of curvatures.

Return loss (S11) is illustrated in Figure 9. We obtain a very low return loss, -7.6 dB, at frequency 4.278 GHz for radius of curvature 20 mm.

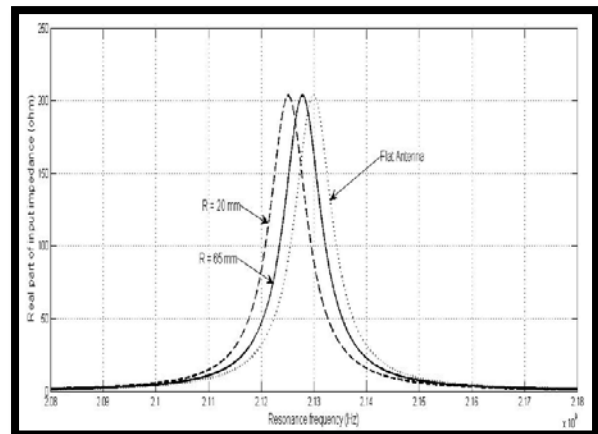
## 5.2. Epsilam-10 Ceramic-Filled Teflon

Figure 10 shows the effect of curvature on resonance frequency for a  $TM_{01}$  mode. The frequency range of resonance frequency due to changing in curvature is from 2.11 to 2.117 GHz for a radius of curvature from 6 mm to flat antenna. So, the frequency is shifted by 7 MHz due to changing in curvature.



**Figure 10.** Resonance frequency as a function of curvature for flat and curved antenna.

Input impedance, real and imaginary parts for a different radius of curvatures are shown in Figures 11 and 12. The peak value of the real part of input impedance is almost 200  $\Omega$  at frequency 2.125 GHz which gives a zero value for the imaginary part of input impedance as shown in Figure 12 at 20 mm radius of curvature. The value 2.125 GHz represents a resonance frequency for the antenna at 20 mm radius of curvature.



**Figure 11.** Real part of the input impedance as a function of frequency for different radius of curvatures.

VSWR is given in Figure 13. It is noted that, the value of VSWR is almost 1.4 at frequency 2.125 GHz which is very efficient in manufacturing process. It should be between 1 and 2 for radius of curvature 20 mm.

Return loss (S11) is illustrated in Figure 14. We obtain a very low return loss, -12 dB, at frequency 2.125 GHz for radius of curvature 20 mm.

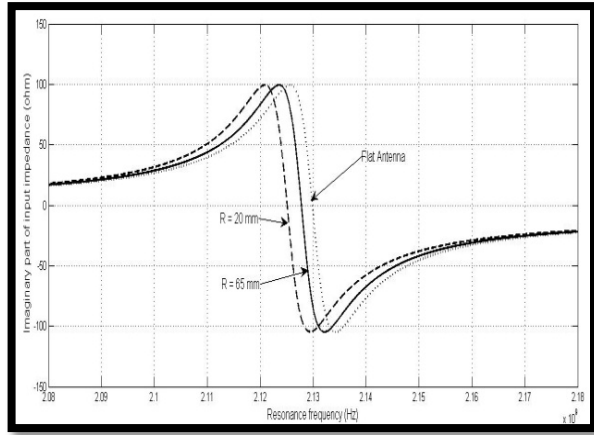


**Figure 12.** Imaginary part of the input impedance as a function of frequency for different radius of curvatures.

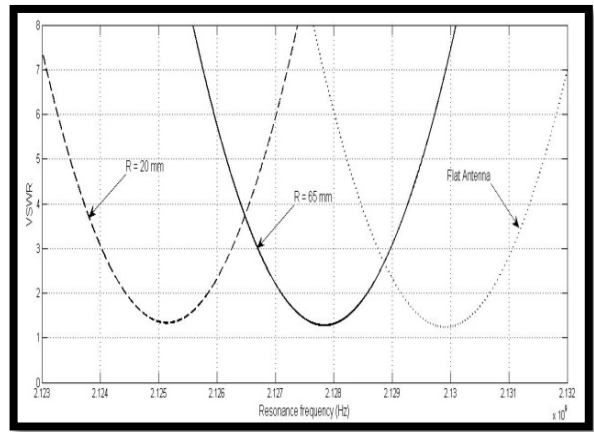


**Figure 13.** VSWR versus frequency for different radius of curvatures.

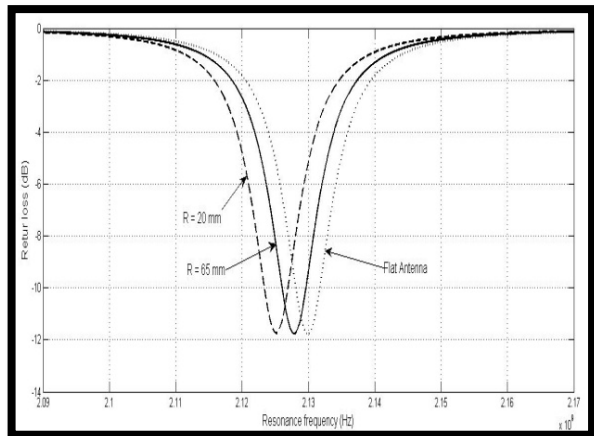


**Figure 14.** Return loss (S11) as a function of frequency for different radius of curvatures.

## 6. Conclusions

The effect of curvature on the input impedance, return loss and voltage standing wave ratio of conformal microstrip antenna on cylindrical bodies for  $TM_{01}$  mode is studied in this paper. Curvature affects the fringing field and fringing field affects the antenna parameters. The Equations for real and imaginary parts of input impedance, return loss,

VSWR and electric and magnetic fields as functions of curvature and effective dielectric constant are derived.

By using these derived equations, we introduced the results for different dielectric conformal substrates. For the two dielectric substrates, the decreasing in frequency due to increasing in the curvature is the trend for all materials and increasing the radiation pattern for electric and magnetic fields due to increasing in curvature is easily noticed.

We conclude that, increasing the curvature leads to increasing the effective dielectric constant, hence, resonance frequency is increased. So, all parameters are shifted toward increasing the frequency with increasing curvature. The shift in frequency is 20 MHz and 7 MHz for K-6098 Teflon/Glass and Epsilam-10 Ceramic-Filled Teflon respectively.

## REFERENCES

- [1] Heckler, M.V., et al., CAD Package to Design Rectangular Probe-Fed Microstrip Antennas Conformed on Cylindrical Structures. roceedings of the 2003 SBMO/IEEE MTT-S International, Microwave and Optoelectronics Conference, p p. 747-757, 2003
- [2] Q. Lu, X. Xu, and M. He, Application of Conformal FDTD Algorithm to Analysis of Conically Conformal Microstrip Antenna. IEEE International Conference on Microwave and Millimeter Wave Technology, ICMMT. , April 2008. p p. 527 – 530, 2008
- [3] Wong, K.L., Design of Nonplanar Microstrip Antennas and Transmission Lines. 1999: John & Sons, Inc
- [4] Josefsson, L. and P. Persson, Conformal Array Antenna Theory and Design 1ed. 2006: Wiley-IEEE Press
- [5] Thomas, W., R.C. Hall, and D. I. Wu, Effects of curvature on the fabrication of wraparound antennas IEEE International Symposium on Antennas and Propagation Society, pp. 1512-1515, 1997
- [6] J. Byun, B. Lee, and F.J. Harackiewicz, FDTD Analysis of Mutual Coupling between Microstrip Patch Antennas on Curved Surfaces. IEEE International Symposium on Antennas and Propagation Society, pp. 886-889, 1999
- [7] Balanis, C.A., AntennaTheory. 2005, New York: John Wiley & Sons
- [8] Pozar, D., Microstrip Antennas. IEEE Antennas and Propagation Proceeding, 1992
- [9] Krown, C.M., Cylindrical-Rectangular Microstrip Antenna. IEEE Trans. on Antenna and Propagation, AP-31: pp. 194-199, 1983
- [10] Q. Wu, M. Liu, and Z. Feng, A Millimeter Wave Conformal Phased Microstrip Antenna Array on a Cylindrical Surface. IEEE International Symposium on Antennas and Propagation Society, pp. 1-4, 2008
- [11] J. Ashkenazy, S. Shtrikman, and D. Treves, Electric Surface Current Model for the Analysis of Microstrip Antennas on Cylindrical Bodies. IEEE Trans. on Antenna and Propagation,

- AP-33: pp. 295-299, 1985
- [12] K. Luk, K. Lee, and J. Dahele, Analysis of the Cylindrical-Rectangular Patch Antenna. IEEE Trans. on Antenna and Propagation. 37: pp. 143-147, 1989
- [13] S. Lei, et al., Anti-impact and Over-loading Projectile Conformal Antennas for GPS,. EEE 3rd International Workshop on Signal Design and Its Applications in Communications, pp. 266-269, 2007
- [14] Kolev, N.Z., Design of a Microstrip Conform GPS Patch Antenna. IEEE 17th International Conference on Applied Electromagnetic and Communications, pp. 201-204, 2003
- [15] A. Elrashidi, K. Elleithy, and Hassan Bajwa, "The Fringing Field and Resonance Frequency of Cylindrical Microstrip Printed Antenna as a Function of Curvature," International Journal of Wireless Communications and Networking (IJWCN), Jul.-Dec., 2011
- [16] A. Elrashidi, K. Elleithy, and Hassan Bajwa, "Effect of Temperature on the Performance of a Cylindrical Microstrip Printed Antenna for  $TM_{01}$  Mode Using Different Substrates," International Journal of Computer Networks & Communications (IJCNC), Jul.-Dec., 2011
- [17] A. Elrashidi, K. Elleithy, and Hassan Bajwa, "The Performance of a Cylindrical Microstrip Printed Antenna for  $TM_{10}$  Mode as a Function of Temperature for Different Substrates," International Journal of Next-Generation Networks (IJNGN), Jul.-Dec., 2011